Dalton Transactions

Accepted Manuscript

ROYAL SOCIETY OF CHEMISTRY

www.rsc.org/dalton

Dalton Transactions

RSCPublishing

ARTICLE

Synthesis, Structure, and Catecholase Activity of Bispyrazolylacetate Copper(II) Complexes

Cite this: DOI: 10.1039/x0xx00000x

Małgorzata J. Gajewska,[a] Wei-Min Ching,[a] Yuh-Sheng Wen[a] and Chen-Hsiung Hung[a*]

Received 00th January 2012,
Accepted 00th January 2012

DOI: 10.1039/x0xx00000x

www.rsc.org/

A series of six-coordination copper(II) complexes containing *bis*(3,5-di-*t*-butylpyrazol-1-yl)acetate (bdtbpza) and *N*-heterocycles or chelating aliphatic ligands have been synthesized. The steric bulkiness of *bis*(pyrazol-1-yl)acetate anchors two bdtbpza to situate a *trans* position and to adopt an *O*-bound monodentate coordination mode with other nitrogen bases occupying the basal plane. Five mononuclear mixed ligand complexes, $[Cu(bdtbpza)_2(py)_4]$ **1**, $[Cu(bdtbpza)_2(^{t\text{-Bu}}py)_4]$ **2**, $[Cu(bdtbpza)_2(pym)_2(MeOH)_2]$ **3**, $[Cu(bdtbpza)_2(eda)_2]$ **4**, $[Cu(bdtbpza)_2(tmeda)(H_2O)_2]$ **5**, where py = pyridine, $^{t\text{-Bu}}$py = *tert*-butylpyridine, pym = pyrimidine, eda = ethylenediamine, and tmeda = tetramethylethylenediamine, were isolated and thoroughly characterized. Intriguingly, the heteroleptic complex **5**, which has two aquo-ligands oriented in the *cis* positions, demonstrates higher catecholase-like activity in performing aerial oxidation of 3,5-di-*tert*-butylcatechol (3,5-DTBC) to 3,5-di-*tert*-butylquinone (3,5-DTBQ) than other *bis*(pyrazolyl)acetate-embedded copper complexes reported herein, which suggests the essential role of labile *cis*-aquo ligands to promote the catalytic reaction.

Introduction

Copper is crucial to all organisms living in oxygen-rich environments. It is present in the active sites of many metalloenzymes and metalloproteins[1] and is involved in oxygen transport, oxygenation reactions, electron transfer, and nitrite reduction.[2] Moreover, several reports brought to attention its antibacterial, antiviral and anti-inflammatory activities.[3] Studies have also revealed the potential use of copper-based compounds as antitumor agents.[4] Additional applications of copper complexes include catalytic chemical bond activation[5] and the supra-molecular assembly of copper ions.[6] Studying the fundamental nature of metal–metal interactions in copper complexes,[7] as well as the correlations between structure and spectroscopic or magnetic behaviour[8] are also very important.

In recent years, metal complexes of scorpionate ligands were successfully adopted to mimic the active sites of metalloenzymes.[9] Scorpionate ligands act as spectator ligands to modulate the electronic and steric properties of the complexes but are not directly involved in the reactions. The azole rings of these ligands are considered as good in mimicking the function of the histidine residues in metalloenzymes. As an example, the scorpionate ligand tris(pyrazolyl)borate was effectively used to construct the μ-η2:η2 peroxo dinuclear copper(II) complexes for elucidating the active site structure of oxyhemocyanin.[10]

Accompanied with the awareness that the 2His1Carboxylate facial triad is a common ligand motif in the active site of metalloenzymes,[11] the coordination compounds containing N,N,O facial tridentate ligands are developed for decoding the electronic structure and reaction mechanisms of non-heme metalloenzymes.[12] The ligand bis(pyrazolyl)acetate which was firstly reported by Otero and co-workers in 1999 appears to be an ideal selection of mimicking 2His1Carboxylate facial triads.[13] To circumvent the common coordination saturation caused by multi-ligand chelation, bulky substituents were appended to the 2,4-positions of pyrazolyl rings to provide steric constrains.[14] Noticeably, in comparison with the comprehensive studies on the coordination chemistry of tris(pyrazolyl)borate, the chemistry using bis(pyrazolyl)acetate derivatives as the ligand is limitedly explored.[15] In order to gain insights into the coordination chemistry of sterically bulky bis(pyrazolyl)acetate ligands, particularly focusing on mixed ligand systems with the presence of a competitive nitrogen base, we have synthesized and structurally characterized a series of heteroleptic six-coordinated copper(II) complexes containing *bis*(3,5-di-*t*-butylpyrazol-1-yl)acetate (bdtbpza) and N-heterocycles or aliphatic bases as the ligands. Interestedly, in all structures the octahedron complexes contain two bdtbpza ligands adopting a monodentate O-bound chelation mode situated at the axial positions with nitrogen bases and solvent molecules chelating at the basal plane. These copper(II)

bdtbpza complexes exhibit moderate catecholase-like activities while $[Cu(bdtbpza)_2(tmeda)(H_2O)_2]$ with a tetramethylethylenediamine and *cis* aquo ligands at the equatorial positions gives a much higher catcholase-like activity. The significance of the ligand arrangement to the catalytic activity is discussed.

Results and discussion

Synthesis

The ligand *bis*(3,5-di-*tert*-butylpyrazol-1-yl)acetic acid (bdtbpza) was prepared according to reported procedures.[14d] A mixture of bdtbpza and copper(II) acetate monohydrate in a 1:2.1 molar ratio in MeOH treated with an excess amount of base, namely pyridine (**1**), *tert*-butylpyridine (**2**), pyrimidine (**3**), ethylenediamine (**4**), or tetramethylethylenediamine (**5**) led to formation of new mononuclear copper complexes **1-5** as shown in Fig 1. All complexes, isolated in good yields and with high purities, were characterized by UV–Vis, FT-IR and EPR spectroscopic studies. The complexes were further studied by ESI-mass spectrometry and thermogravimetric analysis (TGA) to demonstrate the stability and purity. (See ESI) Taking the results of complex **5** as an example, the observed molecular mass with a m/z = 1011.6828 is in agreement with a formula of $[M-2(H_2O)+H]^+$ while the TGA study on complex **5** reveals a stability up to 200 °C without any decline on mass percentage. The structures of all complexes were corroborated by their single crystal structural determinations.

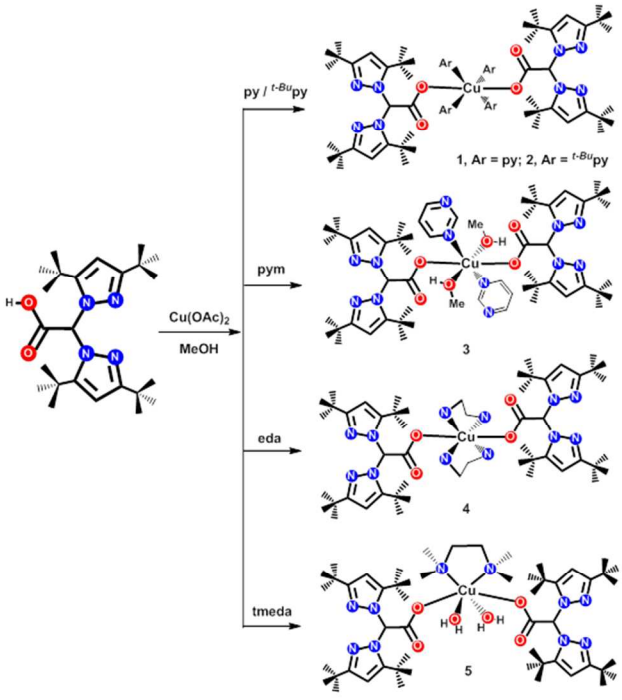

Fig 1. Synthetic outlines for complexes **1-5**

Infrared spectra

The vibrational assignments of the Cu(II) complexes were compared with the corresponding vibrations of the starting materials. All obtained copper compounds exhibit a similar spectral pattern. (see Fig. SI 1 and SI2 in the ESI†) The intense band at 1757 cm^{-1} which corresponds to an asymmetric $\nu_{as}(COO)$ stretch mode of the free bdtbpza ligand is shifted considerably to lower frequencies by ca. 100-140 cm^{-1} indicating coordination through the carboxylate group. The bands located at around 1360 cm^{-1} are assigned to symmetric carboxylate stretch mode $\nu_{sym}(COO)$. The differences (Δ) between asymmetric and symmetric frequencies, $\Delta[\nu_{as}(COO)-\nu_{sym}(COO)]$, for compounds **1-5**, vary between 260–295 cm^{-1} and indicate an O-bound monodentate coordination mode for bdtbpza.[16,17]

Electronic spectra

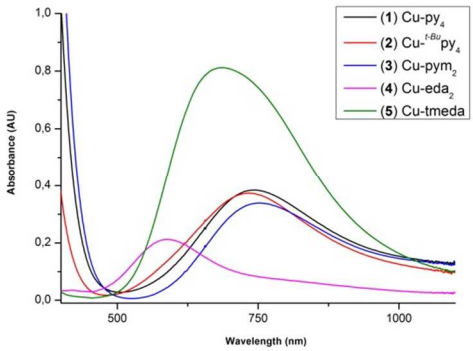

Fig. 2 Electronic absorption spectra of complexes **1-5** ($5x10^{-3}$ M in CH_2Cl_2).

For Cu(II) complexes, as a result of distortion of octahedral geometry, the ^2E_g and $^2T_{2g}$ levels are split into $^2B_{1g}/^2A_1g$, and $^2B_{2g}/^2E_g$ states, respectively. In undistorted octahedral coordination, only a single electronic transition occurs, whereas, due to Jahn-Teller effect, three transitions corresponding to $^2B_{1g}\rightarrow{}^2A_{1g}$, $^2B_{1g}\rightarrow{}^2B_{2g}$, and $^2B_{1g}\rightarrow{}^2E_g$, should be observed, although more commonly their weak and broadened characters as well as close in energies make them appear as one broad envelope. The absorption spectra of all studied compounds **1-5** are depicted in Fig. 2. The ^2E_g and $^2T_{2g}$ states of the octahedral Cu(II) (d^9) remain unresolved and, in all spectra, all three transitions, $^2B_{1g}\rightarrow{}^2B_{2g}$, $^2B_{1g}\rightarrow{}^2E_g$ and $^2B_{1g}\rightarrow{}^2A_{1g}$ lie within the single broad envelope centred at 13,399–17,182 cm^{-1}. Nevertheless, the nature of the donor ligands in the equatorial plane of the coordination sphere results in some subtle differences in the position and the maximum absorption intensity of the d-d bands. The d-d absorption band with molar extinction coefficient (ε) of 162 $L{\cdot}mol^{-1}{\cdot}cm^{-1}$ for complex **5** containing tmeda chelating ligand is much stronger than in other compounds. The ε values of λ_{max} for discussed complexes increase in the following order 4 < 3 < 2 < 1 << 5. (Table 1) Complex **5**, [Cu-tmeda], has a higher extinction coefficient due to its lower symmetry and higher degree of distortion from ideal octahedral centrosymmetric geometry.

Table 1 Electronic spectral data of compounds 1-5

Comlexes		λ_{max}	10^3 cm^{-1}	ε
[Cu-py]	**1**	744	13.44	77
[Cu-$^{t\text{-Bu}}$py]	**2**	734	13.62	75
[Cu-pym]	**3**	754	13.26	68
[Cu-eda]	**4**	590	16.45	42
[Cu-tmeda]	**5**	689	14.51	162

EPR spectra

The EPR spectra of complexes **1-5** were recorded in CH_2Cl_2 at room temperature and as frozen solutions at 77K. The room temperature spectra for compounds with bdtbpza and N-heterocyclic ligands (**1**, **2** and **3**) showed semi-isotropic patterns with no clearly resolved hyperfine splitting. In contrast, the splitting in the room temperature spectra of **4** and **5** is clearly visible (see Fig. SI 3a and SI 4a in the ESI†). The EPR spectra recorded at 77K in frozen CH_2Cl_2 shows axial pattern consisting of four well-defined hyperfine lines due to coupling with copper nuclei in the parallel region. The parameters of spectra are comparable to those of reported complexes containing a CuN_4O_2 or CuN_2O_4 coordination sphere.[18] The obtained values of $g_{\|}$ and $g_{\perp}$ shown in Table 2 for the complexes display the order $g_{\|}>g_{\perp}>2.0023$, which is consistent with a $^2B_{1g}$ (d_{x2-y2}) ground state,[19] a character of axially elongated mononuclear copper(II) complexes. According to Kivelson and Neiman,[19] M-L bonds in compounds with $g_{\|} \geq 2.3$ are ionic in nature, while those with $g_{\|} \leq 2.3$ reveal covalent character. Applying these criteria, the covalent character of the metal-ligand bond in the complexes **1-5** can be predicted. The EPR spectra **1-5** at 77 K showed well-defined hyperfine splitting on the low-field region with $A_{\|}$ values in the range of 2600-3200 gauss. However in the perpendicular region $B_{\perp}$, the super-hyperfine splitting, due to interaction with ^{14}N (I = 1) provided by amine ligands, is not observed. The parallel hyperfine coupling between the unpaired electron and the copper nuclear spins ($A_{\|}$) is affected by the donor properties of N-heterocycle or aliphatic amines coordinated to metal center. The $A_{\|}$ values were observed to be 160×10^{-4} cm^{-1}, 189×10^{-4} cm^{-1} 169×10^{-4} cm^{-1}, 202×10^{-4} cm^{-1} and 171×10^{-4} cm^{-1}, for $[CuL_2(py)_4]$ (**1**), $[CuL_2(t\text{-Bupy})_4]$ (**2**) and $[CuL_2(pym)_2(MeOH)_2]$ (**3**), $[CuL_2(eda)_2]$ (**4**), $[CuL_2(tmeda)(H_2O)_2]$ (**5**), respectively. We noticed that a decrease on the value of $g_{\|}$ accompanies an increase of $A_{\|}$. The lower $g_{\|}$ and the higher $A_{\|}$ values implying a ligand field strengthening of the copper in-plane coordination. The relatively high values of $A_{\|}$, varying in the range of 160-202 x 10^{-4} cm^{-1} suggests small axial interaction.[20]

The EPR spectra in compounds **1-5** were simulated to get accurate values of various parameters (Table 2; see Fig. SI 3b and SI 4b in the ESI†). The average value of the hyperfine splitting tensor, A_{av}, and average g value, g_{av}, were calculated using expressions: $A_{av} = (A_{\|} + 2A_{\perp})/3$ and $g_{av} = (g_{\|} + 2g_{\perp})/3$, respectively. In the elongated octahedron, the value of α^2, which can be regarded as measure of covalency of the in-plane σ-bonds in Cu(II) systems, is given by the Kivelson and Neiman equation:

$$\alpha^2 = [(A_{\|} / 0.036)] + (g_{\|} - 2.0023) + 3/7(g_{\perp} - 2.0023) + 0.04$$

This value lies between 0.5 for pure covalent bonding and 1 for pure ionic bonding. The α^2 values in the range 0.79 – 0.85 for complexes **1-5** suggest that the metal ligand bonds have an intermediate character with similar contributions of both ionic and covalent interactions. In axial symmetry, the g value is related to the geometric parameter G by an expression $G = (g_{\|}-2)/(g_{\perp}-2)$ and the G value can be used to gauge the exchange interaction between copper(II) centers in the polycrystalline state. The complexes in the present study show G values higher than 4 (Table 2), which indicate absence of any Cu-Cu interaction in the complex.[21] Finally, the empirical factor f(α), where $f(\alpha) = g_{\|}/A_{\|}$, is an index of tetragonal distortion and shows deviation from idealized geometry. Values between 110–120 are typical for planar complexes, while within the range of 130–150 are characteristic of slight to moderate distortion, and 180–250 indicate considerable distortion.[22] The value from 119-145 for titled complexes indicate small to moderately distorted geometry.

Structural analysis of copper complexes 1-5

The crystal structures the copper(II) complexes **1-5** were unambiguously established by single crystal X-ray structural determinations. The structural data for all complexes are summarized in Table 3. Earlier reports demonstrated the anticipated κ^3-N,N,O coordination mode of *bis*(pyrazol-1-yl)acetate ligation to metal centre.[23] However, we found that application of strong electron-donating co- ligands, such as pyridine or ethylenediamine, influences the chelation modes of bdtbpza ligand to copper(II) ions and thus regulates the final structures of the title compounds **1-5**. In our system, the

Table 2 Spin Hamiltonian and bonding parameters for copper complexes

compound	(**1**)	(**2**)	(**3**)	(**4**)	(**5**)
$g_{\|}$	2.323	2.250	2.316	2.190	2.260
$g_{\perp}$	2.058	2.037	2.057	2.024	2.039
g_{av}	2.146	2.108	2.143	2.079	2.113
$A_{\|}$ [10^{-4} cm^{-1}]	160	189	169	202	171
$A_{\perp}$ [10^{-4} cm^{-1}]	17	20	19	29.4	21
A_{av} [10^{-4} cm^{-1}]	64	76	69	87	71
G	5.57	6.76	5.54	7.92	6.67
α^2	0.83	0.83	0.85	0.80	0.79
f	145	119	137	108	132

Table 3 Crystal data and refinement for the copper complexes **1-5**

Compound	**(1)**	**(2)**	**(3)**	**(4)**	**(5)**
Empirical formula	$C_{73}H_{107}CuN_{13}O_6$	$C_{90}H_{154}CuN_{12}O_{10}$	$C_{58}H_{94}CuN_{12}O_6$	$C_{52}H_{106}CuN_{12}O_{10}$	$C_{55}H_{102}CuN_{10}O_7$
Formula weight	1326.25	1627.79	1118.99	1123.03	1079.00
Crystal system	Triclinic	Monoclinic	Monoclinic	Monoclinic	Orthorhombic
Space group	P-1	P2(1)/c	P 2(1)/n	P2(1)/c	Pccn
a/Å	10.4227(4)	15.7877(9)	10.3932(4)	10.945(2)	31.3645(5)
b/Å	13.0591(7)	18.5432(12)	20.4318(7)	31.194(6)	10.4436(2)
c/Å	15.0888(6)	17.9411(11)	32.1985(13)	18.956(4)	18.7587(2)
α/ °	79.592(4)	90	90	90	90
β/ °	89.648(3)	114.444(4)	98.685(2)	100.60(3)	90
γ/ °	66.674(3)	90	90	90	90
Unit cell volume/$Å^3$	1850.00(14)	4781.5(5)	6759.0(4)	6361(2)	6144.57(17)
Z	1	2	4	4	4
Temperature/ K	100.00(10)	100.00(10)	200(2)	200(2)	100.00(10)
μ/ mm	0.345	0.287	0.375	0.403	0.411
λ/ Å (MoKα)	0.71073	0.71073	0.71073	0.71073	0.71073
Reflection measured	55237	60281	45917	43553	56787
Reflection total	6999	9795	11981	11181	6780
R_1 [$I > 2\sigma(I)$]	0.0664	0.0768	0.0972	0.0737	0.0646
w$R(F^2)$ [$I > 2\sigma(I)$]	0.1904	0.1652	0.2150	0.2006	0.1956
GOF	0.984	1	1.153	1.038	1.043

bdtbpza ligand coordinates to the metal ion in a monodentate O-bound fashion. Except for complex **5**, which exhibits trigonal prismatic distortion, the described compounds have two bdtbpza ligands situated at a *trans* orientation to each other occupying the axial positions of the N_4O_2 or N_2O_4 coordination sphere. Other ligated bases have occupied the equatorial positions to complete complexes with a distorted octahedral geometry. In all complexes the *bis*(pyrazolyl)acetate ligands are not planar. The average dihedral angles between the two pyrazole rings for **1-5** are 88.4º, 89.2º, 82.3º, 87.6º, 85.4º, respectively. As usual for octahedrally coordinated copper(II) ions, the Jahn-Taller distortion occurs and results in marked tetragonal distortion to give an elongated Cu-O bond for two axial bdtbpza ligands. Despite the obvious similarities, differences between the respective coordination modes were found and were summarized below.

$Cu(BDTBPZA)_2(PY)_4$] (1). Selected bond distances and angles for this compound are outlined in Table 4, while the structure is depicted in Fig. 3. Complex **1** crystallizes in triclinic P-1 space group with the Cu(II) ion located at the centre of symmetry. As shown in Figure 3, the distances 2.006(4) and 2.066(4) Å for Cu−N(1) and Cu−N(2), respectively, are normal distances for

Cu−N bonds while the distance of Cu−O(1), from copper ion to the oxygen atom of bdtbpza ligand, has been elongated to 2.449(4) Å. The O(2) atoms do not coordinate to the copper ion, as suggested by a long Cu-O(2) separation of 4.083(3) Å.

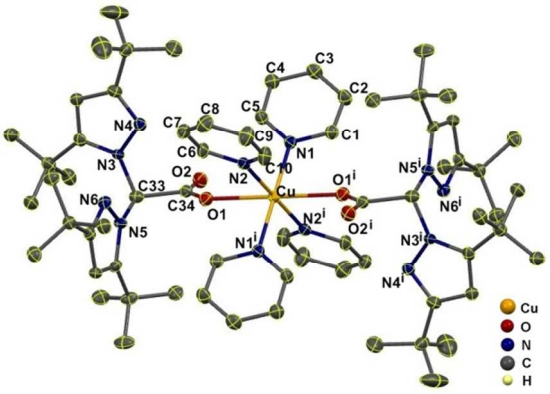

Fig. 3 Crystal structure of $[Cu(bdtbpza)_2(py)_4]$ (1) showing the atom numbering scheme; hydrogen atoms and co-crystallized solvent molecules are omitted for clarity.

Table 4 Selected bond distances (Å) and angles (°) refer to **1** and **2**

Compound **1**			
Cu-N(1)	2.006(4)	$N(1)^i$-Cu-N(2)	88.19(14)
Cu-N(2)	2.066(4)	N(1)-Cu-N(2)	91.81(14)
Cu-O(1)	2.449(3)	N(1)-Cu-$N(1)^i$	180.0(1)
Cu-O(2)	4.083(3)	O(1)-Cu-$O(1)^i$	180.0(1)
Compound **2**			
Cu-N(5)	2.000(4)	N(5)-Cu-$N(6)^i$	87.29(16)
Cu-N(6)	2.055(4)	N(5)-Cu-N(6)	92.71(16)
Cu-O(1)	2.487(2)	$N(5)^i$-Cu-N(5)	180.00(1)
Cu-O(2)	4.103(3)	O(1)-Cu-$O(1)^i$	180.0(1)

Table 5 Distances (Å) and angles (°) relevant to hydrogen bonds in complex **2**

D−H···A	d(D−H)	d(H···A)	d(D···A)	<(DHA)
[Cu-$^{t\text{-Bu}}$py] (**2**)				
O3−H(3)···$O2^{ii}$	0.847	1.866	2.688	163.12
O4−H(4)···$O2^{ii}$	0.880	1.932	2.797	167.30
O5−H(5)···$O3^{ii}$	0.836	2.120	2.844	144.85

Equivalent positions: (i): x, +y+1, +z; (ii): x, y, z;

The dihedral angle between the two planes formed by two pyridine rings diagonal to each other has an angle of 83.43°. The crystal structure is stabilized by short non-bonding contacts (3.072 Å) between pyrazole nitrogen atoms N4···N6.

[Cu(bdtbpza)$_2$(t-Bupy)$_4$] (2). The title complex crystallizes in the monoclinic space group $P2_1/c$. As shown in Figure 4 and Table 4, complex **2** is isostructure of **1** with an N_4O_2 octahedron coordination sphere formulated by four nitrogen atoms belonging to four *tert*-butylpyridine rings in the basal plane and two oxygen atoms from monodentate bdtbpza ligands. The Cu−N distances, 2.000 Å and 2.055 Å, contrast with the elongated Cu−O bonds (2.487 Å) in the axial position. The high symmetry of molecule is reflected in 180° bond angles for $N(5)^i$−Cu−N(5), $N(6)^i$−Cu−N(6), and $O(1)$−Cu−$O(1)^i$. The basal angles of 87.29(16) and 92.71(16)° are close to the ideal value of 90° (Table 1).

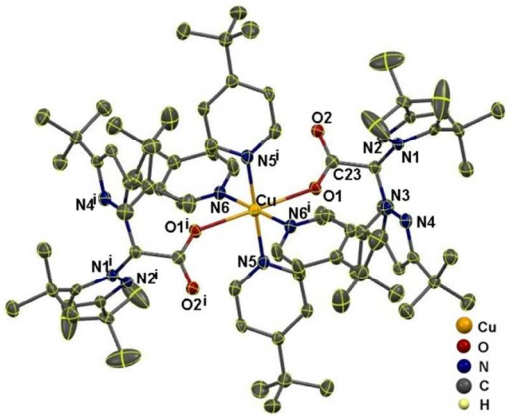

Fig. 4 Crystal structure of $[Cu(bdtbpza)_2(^{t\text{-Bu}}py)_4]$ (**2**) showing the atom numbering scheme; hydrogen atoms and co-crystallized solvent molecules are omitted for clarity.

The molecular structures of the complex **2** are stabilized by extensive O−H···O hydrogen bonds among cocrystallized MeOH molecules and bdtbpza ligands. The hydrogen bonding occurs through O(3)−H(3)···O(2) and O(4)−H(4)···O(2) interactions with O···O distances of 2.688(5) Å and 2.797(6) Å, respectively. Moreover, the weak intermolecular hydrogen bonding between two solvated methanol molecules are also found (see Table 5 and Fig. 5).

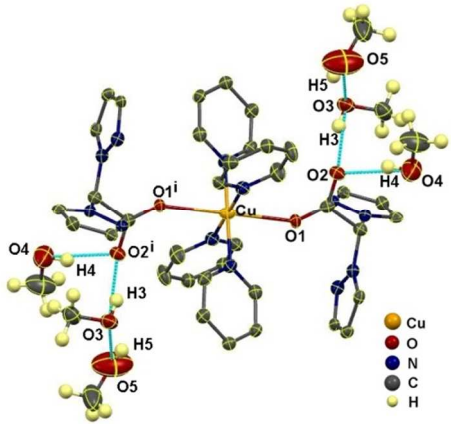

Fig. 5 The hydrogen bonds formed by the lattice methanol molecules in compound $[Cu(bdtbpza)_2(t\text{-Bupy})_4]$ (**2**). Hydrogen bonds are indicated by blue lines, t-Bu group and H atoms are omitted for clarity.

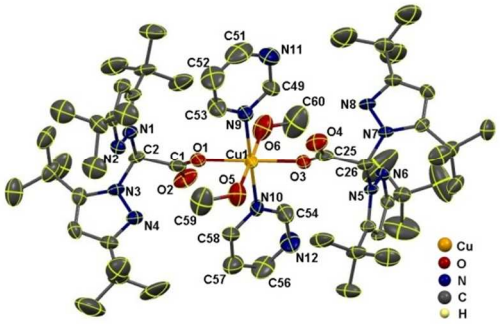

Fig. 6 Crystal structure of $[Cu(bdtbpza)_2(pym)_2(CH_3OH)_2]$ (**3**) with atom numbering scheme; hydrogen atoms are omitted for clarity.

$Cu(bdtbpza)_2(pym)(CH_3OH)_2]$ (3). Complex **3** crystallized in the monoclinic space group $P2_1/n$ with four formula units in the unit cell. The molecular structure of **3** is analogous to the above ones. However, in this case, the copper atom is best described as a distorted octahedral N_2O_4 coordination environment. As shown in Fig. 6, each molecule of the same type is in *trans* positions to another.

Interestingly, in this structure, the basal plane is defined by two oxygen atoms (O1, O3) of two heteroscorpionate ligands and two nitrogen atoms (N9, N10) from two pyrimidine molecules. The octahedron is completed at the axial positions by two oxygen atoms (O5 and O6) from two methanol molecules at the elongated bond distances of 2.416(4) Å for Cu(1)−O(5) and 2.466(4) Å for Cu(1)−O(6). The Cu−O and Cu−N distances are comparable to reported complexes with the same CuN_2O_4 coordination sphere.[24] Since situated in the basal plane, as listed in Table 6, the distances between metal center and both oxygen atoms of the bdtbpza carboxylate group are much shorter than in the cases of **1** or **2**.

Table 6 Selected bond distances (Å) and angles (°) for **3**

Compound **3**			
Cu(1)-N(9)	2.035(4)	O(1)-Cu(1)-O(3)	179.39(15)
Cu(1)-N(10)	2.034(4)	N(9)-Cu(1)-O(5)	90.9(2)
Cu(1)-O(1)	1.957(3)	N(10)-Cu(1)-O(5)	90.5(2)
Cu(1)-O(3)	1.958(3)	N(9)-Cu(1)-O(6)	89.8(2)
Cu(1)-O(5)	2.416(4)	N(10)-Cu(1)-O(6)	88.8(2)
Cu(1)-O(6)	2.466(4)	O(1)-Cu(1)-N(9)	87.39(16)
Cu(1)-O(2)	3.436(4)	O(1)-Cu(1)-N(10)	92.93(15)
Cu(1)-O(4)	3.448(4)		

$[Cu(bdtbpza)_2(eda)_2]$ (4). Crystallographic analysis of **4** shows that the copper is chelated by two ethylenediamine (eda) ligands while the fifth and sixth positions of an octahedron are occupied by one oxygen from carboxylic group of each bdtbpza ligand as shown in Fig 7. The terminal nitrogen atoms of each eda molecule created five-member chelated rings with two longer and two slightly shorter Cu−N(amine) bond lengths (2.013(4)/2.014(5) Å and 2.002(4)/1.997(4) Å, respectively; Table 7). Both Cu−N distances and the small N−Cu−N bite angles for five-membered MN2C2 chelating rings (85.0º, 85.2º) are within the normal range for copper complexes with N,N-chelating ligands.[24-25] The chelated eda rings adopt gauche configuration with the C49, C50, C51, and C52 atoms deviating to either side of the plane of the near coplanar coordination squares CuN_4 by 0.38, -0.36, 0.28, and -0.34 Å, respectively. The Cu(1)−O(1) (2.536 (3) Å) and Cu(1)−O(3) (2.450(3) Å) bonds are much longer than Cu−N bonds in basal plane and are comparable with those in related Cu(eda)-type complexes.[26] The maximum deviation from the ideal octahedral angle is found for the angle O(1)−Cu(1)−N(12) 80.9(2)°.

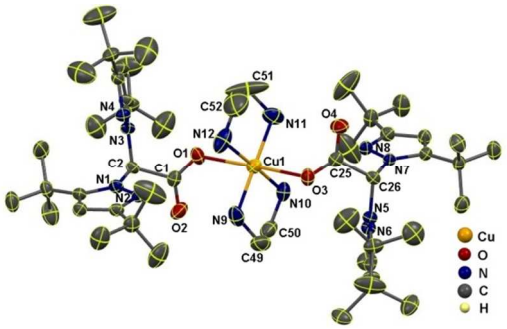

Fig. 7 Molecular structure of complex $[Cu(bdtbpza)_2(eda)_2]$ (**4**) with atom numbering scheme; hydrogen atoms are omitted for clarity.

$[Cu(bdtbpza)_2(tmeda)(H_2O)_2]$ 5. Complex **5** crystallizes in an orthorhombic crystal system with Pccn space group. Important bond distances and angles are listed in Table 7, while Fig. 8 shows molecular structure and hydrogen-bonding interactions. The mononuclear complex consists of a copper(II) center in a trigonal prismatic distorted CuN_2O_4 environment. The metal ion is surrounded by two O-bound bdtbpza ligands, nitrogen atoms of 1,2-diamine ligand, as well as oxygen atoms from two

Table 7 Selected bond distances (Å) and angles (°) refer to **4** and **5**

Compound **4**			
Cu(1)-N(9)	2.002(4)	O(1)-Cu(1)-O(3)	178.1(1)
Cu(1)-N(10)	2.013(4)	N(12)-Cu(1)-N(11)	85.0(2)
Cu(1)-N(11)	1.997(4)	N(10)-Cu(1)-N(11)	95.4(2)
Cu(1)-N(12)	2.014(5)	N(12)-Cu(1)-N(9)	94.5(2)
Cu(1)-O(1)	2.536(3)	N(10)-Cu(1)-N(9)	85.17(19)
Cu(1)-O(3)	2.450(3)	N(11)-Cu(1)-N(9)	178.34(19)
Cu(1)-O(2)	3.798(4)	N(12)-Cu(1)-N(10)	176.12(18)
Cu(1)-O(4)	3.839(4)		
Compound **5**			
Cu−N(29)	2.301(2)	O(1)-Cu-O(3)	83.24(7)
Cu−O(1)	2.1795(18)	O(1)-Cu-O(3)^{i}	82.34(7)
Cu−O(3)	2.1814(19)	O(1)-Cu-O(1)^{i}	155.63(10)
Cu−O(2)	3.439(2)	O(3)-Cu-O(3)^{i}	107.05(11)
		O(3)-Cu-N(29)	163.44(8)
		O(1)-Cu-N(29)	92.55(7)
		N(29)-Cu-N(29)^{i}	77.66(12)

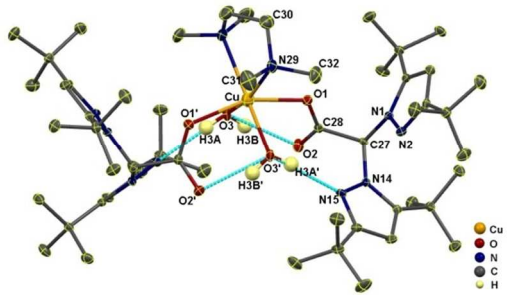

Fig. 8 Molecular structure of complex $[Cu(bdtbpza)_2(tmeda)(H_2O)_2]$ (**5**) with atom numbering scheme together with the hydrogen bonds formed by the lattice water molecules in compound. Hydrogen bonds are indicated by blue lines, H atoms are omitted for clarity.

coordinated water molecules, at the distances of 2.1795(18) Å, 2.301(2) Å and 2.1814(19) Å respectively. These values are relatively similar to those of other complexes with both oxygen and nitrogen atoms coordinated to the copper ion.[27] Unexpectedly, the elongated copper(II)–nitrogen bonds are located at positions *cis* to each other which is in contradiction to traditional compressed or elongated tetragonal distortion resulting from Jahn-Teller effect. In contrary to Cu-eda system in **4** (Fig. 7), only one spacious tmeda ligand can be accommodated in the coordination sphere. (Fig. 8) The trigonal prismatic-type distortion can also be realized from the small bite angle N−Cu−N of 77.66(12)° and unusually large angle of 107.05(11)° for O(3)-Cu-O(3)^{i}. The *trans* angles at the copper(II) ion range from 155.63(10)° for O(1)−Cu−O(1)^{i} to 163.44(8) for O(3)−Cu−N(29), showing significant distortion. Presumably, the structural distortion in complex **5** can be attributed to the strong intramolecular hydrogen bonding interactions between coordinated water molecules and nitrogens of pyrazolyl rings (O−H···N) with an O3−N15 distance of 2.840(3) Å. Water molecule is also involved in hydrogen bond formation with a non-coordinated oxygen of the adjacent bis(pyrazolyl)acetate ligand (Table 8).

Table 8 Distances (Å) and angles (°) relevant to hydrogen bonds in complex **5**

D−H···A	d(D−H)	d(H···A)	d(D···A)	<(DHA)
O3−H(3A)···N15^{i}	0.817	2.027	2.840	172.30
O3−H(3B)···O2^{ii}	0.817	1.899	2.652	152.83

Equivalent positions: (i): x, y, z; (ii): - x+1/2+1, -y+1/2, +z

Tetragonality parameter

The degree of molecular distortion from ideal octahedral geometry can be defined through a tetragonality parameter described as: $T = R_{int}/R_{out}$, where R_{int} and R_{out} are the average in-plane and out-of-plane distances, respectively. This parameter shows whether Jahn-Teller distortion is static ($T < 0.9$) or dynamic ($T = 1$).[28] T values for all hexacoordinated copper (II) complexes are listed in Table 9. As we can see below, complexes **1**, **2**, **3** and **4** have T values less than 0.9, whereas compound **5** has T = 1.0029.

Table 9 The teragonality parameter T of copper (II) complexes **1-5**

complex		chromophore	R_{int}	R_{out}	T[a]
[Cu-py]	(**1**)	CuN_4O_2	2.043	2.447	0.835
[Cu-$^{t\text{Bu}}$py]	(**2**)	CuN_4O_2	2.028	2.487	0.815
[Cu-pym]	(**3**)	CuN_2O_4	1.994	2.442	0.817
[Cu-eda]	(**4**)	CuN_4O_2	2.006	2.492	0.805
[Cu-tmeda]	(**5**)	CuN_2O_4	2.241	2.178	1.029

[a] T is the tetragonality parameter where $T = R_{int}/R_{out}$ (R_{int} and R_{out} are the average in-plane and out-of-plane distances, respectively).

Catechol oxidation activity

Catechol oxidase is a type III copper protein containing a binuclear active site involved in the oxidation of catechols to the highly reactive quinones that undergo auto-polymerization and transform into brown pigment, melanin. Understanding of structural and functional aspects of catechol oxidase has been obtained through the biomimetic modelling of its active site. Several mechanisms and theoretical investigations have been reported for dinuclear copper complex systems. In model studies on catecholase activity, 3,5-di-*tert*-butyl-catechol

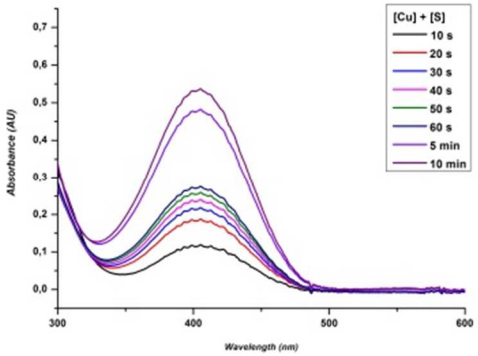

Fig. 9 Time sequence of increase in the absorption band of 3,5-DTBQ in the catechol oxidation reaction catalysed by [Cu-tmeda] (**5**). The reaction were performed in CH_2Cl_2 under air at 22°C, $[Cu\text{-}tmeda]_0=2.6\times10^{-7}$ M and $[3,5\text{-}DTBC]_0=2.6\times10^{-6}$ M, Δt=10 min.

(3,5-DTBC) has been broadly used as a substrate. Owing to its low redox potential, the substrate is easily oxidized and the bulky *t*-butyl substituents prevent further ring-opening reactions after conversion to quinone.[29] The product 3,5-di-*tert*-butyl-*o*-benzoquinone (3,5-DTBQ), is stable and has strong absorption at λ_{max} = 404 nm with an extinction coefficient of 1861 $dm^3mol^{-1}cm^{-1}$ in dichloromethane at 22 °C (see Fig. SI 5 in the ESI†). The catechol oxidation reaction of $[Cu(bdtbpza)_2(tmeda)(H_2O)_2]$ **5** with 3,5-DTBC, was evaluated by means of UV-Vis spectroscopy at 22 °C in air and in dioxygen-saturated dichloromethane by monitoring the increase of absorption band at 404 nm. Control experiments carried out under similar reaction conditions in the absence of a catalyst show no conversion of 3,5-DTBC to the product.

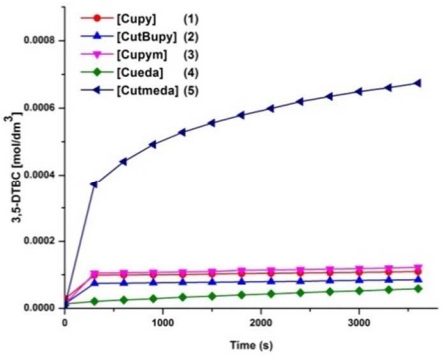

Fig. 10 Time dependent oxidation of 3,5-DTBC ($1.2x10^{-3}$ M) by complexes **1**-**5** ($1.2x10^{-4}$ M).

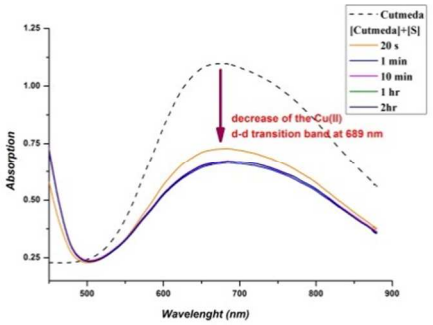

Fig. 11 The reduction of copper(II) center in complex **5** by 3,5-DTBC in anaerobic conditions; [Cu-tmeda]=$5x10^{-3}$ M and [3,5-DTBC]= $5x10^{-3}$ M

We observed that using **5** as the catalyst, oxidation is fast in air and proceeds even more rapidly under dioxygen. This implies that the dioxygen concentration has a significant impact on the rate of the reaction. However, the catalytic process slows down over time, probably due to the influence of accumulated quinone product (3,5-DTBQ).[30] The plot in Fig. 9 demonstrates the formation of quinone, while time-dependent increase in product concentration is shown in Fig. 10. The lowering of the intensity of d−d band centred at 689 nm accompanied (Fig. 11) by the change of the color of the solution from blue to yellow upon mixing the catalyst with the substrate under both aerobic and anaerobic conditions is consistent with an electron transfer process from catechol to the copper(II) center which is subsequently reduced to copper(I).[29] Moreover, the anaerobic interaction of **5** with substrate in a 1:1 mole ratio yielded 18% quinone product according to the absorbance of 3,5-DTBQ at 404 nm from the UV-Vis spectrum. Approximately 33% conversion from Cu(II) to Cu(I) in the same solution based on the falling of d-d band absorbance is consistent with a two electrons oxidation process. Interestingly, the EPR study shows a weak signal at *g* value 1.9807 during the reaction of complex **5** with 3,5-DTBC suggesting the formation of an organic radical species as the reaction intermediate in the catalytic process (Fig. 12). A 57% conversion yield was obtained when a 1:10 mole ratio of [catalyst]/[substrate] was used for the catalytic reaction in air. Noticeably, using $[Cu(bdtbpza)_2(eda)_2]$ (**4**) as the catalyst for the catechol oxidation reaction under the identical conditions gave only metal oxidation and trace amount of product (~ 3% after 1h). The time-dependent product concentration as shown in Fig. 10 also confirms that complex **5** has a higher catalytic activity than complexes **1**-**4**. The difference in activities suggests that two weak aquo ligands coordinating in *cis* position will be substituted by the substrate to allow a more effective inner-sphere electron transfer process and facilitate the catalytic reaction. Additionally, the calculated activity values for the oxidation of 3,5-di-tert- butylcatechol by complex **5** of 7.9 x 10^{-2} μmol per mg of catalyst per min is higher than a typical range of (0.5-1) x 10^{-3} μmol reported in literature.[31]

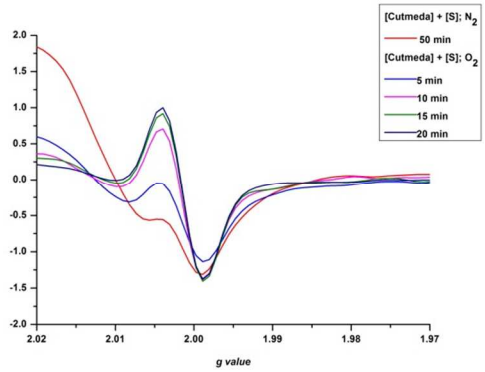

Fig. 12 EPR study of the formation of an organic radical species during the reaction of [Cu-tmeda] with 3,5-DTBC in DCM solution; molar ratio of [Cu-tmeda]:[3,5-DTBC] 1:10, 22°C.

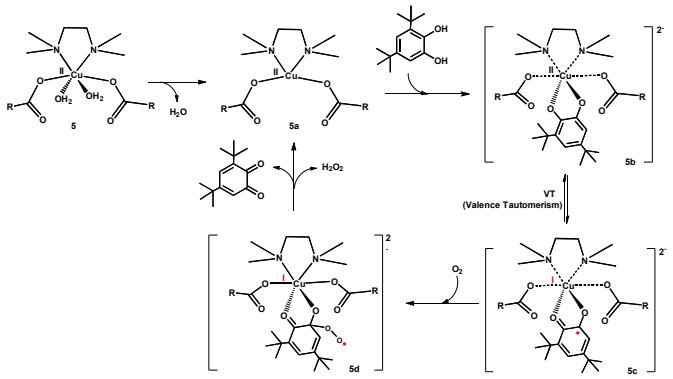

Scheme 1 Proposed mechanism of catechol oxidation catalysed by $[Cu(bdtbpza)_2(tmeda)(H_2O)_2]$ (**5**)

Mechanistic considerations

On the basis of spectroscopic evidence, a mechanism for the catechol oxidation by compound **5**, as depicted in Scheme 1 is proposed. In the first step of the reaction, the dissociation of water molecules takes place and a starting precatalyst (**5a**) is formed. The catechol molecule then coordinates to the precatalyst and forms intermediate complex-substrate adduct (**5b**), which may favor the electron transfer in association with a valence tautomerization and equilibrate between Cu(II)-(3,5-DTBC) (**5b**) and semiquinone (SQ) intermediate Cu(I)-(3,5-DTBSQ) (**5c**).[32] The exact conformation of **5b** and **5c** is still uncertain. The monitoring on this catalytic reaction by mass spectrometer observed a peak with *m/z* value of 815.51 which is

consistent with a copper(I) complex with a formula of [M−*bdtbpza*−2(H_2O)+catechol+H]$^-$. The resulting Cu(I)-(3,5-DTBSQ) (**5c**) molecule reacts with dioxygen creating oxygenated species (**5d**) which oxidizes the Cu(I) center and releases 3,5-DTBQ and hydrogen peroxide. After the quinone molecule is released, the copper catalyst is regenerated and the catalytic cycle can continue.[33]

Conclusions

In this paper, we have described the synthesis of a series of six-coordination copper(II) complexes containing bis(3,5-di-t-butylpyrazol-1-yl)acetate (bdtbpza) and N-heterocycles or chelating aliphatic ligands. The structures of all complexes were confirmed by their single crystal structural determinations. We found that application of strong electron-donating co-ligands, such as pyridine or ethylenediamine, influences the chelation modes of bdtbpza ligand to copper(II) ions and thus regulates the final structures of the title compounds **1-5**. Moreover, the ligand arrangements around metal center provoke significant differences in catalytic activity of **1-5** in performed aerial oxidation of 3,5-di-*tert*-butylcatechol (3,5-DTBC) to 3,5-di-*tert*-butylquinone (3,5-DTBQ). The heteroleptic complex [Cu(bdtbpza)$_2$(tmeda) (H_2O)$_2$] **5** , which has two aquo-ligands oriented in the cis positions, demonstrated higher catecholase-like activity than other bis(pyrazolyl)acetate-embedded copper complexes reported herein.

Experimental

General methods and instrumentation

All experiments were carried out under aerobic conditions. Solvents and commercially available substances were of reagent grade and used without further purification. The ligand bis(3,5-ditertbutylpyrazol-1-yl)acetic acid was prepared based on published procedures.[14d] Elemental analyses for carbon, hydrogen and nitrogen were performed on a Heraeus CHN-OS Rapid Elemental Analyzer. The infrared spectra (4000 ~ 500 cm^{-1}) were recorded on a VERTEX 70 spectrometer by using Golden Gate diamond ATR accessory on solid powder samples. The UV−visible absorption spectra were recorded using a JASCO V-670 UV−vis/NIR spectrophotometer. The low and room temperature EPR spectra were recorded on a Bruker E580 FT/CW EPR spectrometer.

Preparations

Cu(bdtbpza)$_2$(py)$_4$](1). To the solution of Cu(CH_3COO)$_2$•H_2O (50.0 mg, 0.25 mmol) in 4 mL of MeOH the mixture of bdtbpza (228.4 mg, 0.52 mmol) and pyridine (0.5 mL) in 2 mL MeOH was added. The resulting blue solution was stirred at room temperature for 30 min. The blue precipitates formed were filtered off, washed with small amounts of methanol (2 x 2.5mL) and dried under vacuum at ambient temperature for 2 h (250 mg, 78%). Single crystals of **1**, suitable for X-ray structure determination, were obtained by slow evaporation of the filtrate over a week. Elemental analysis (%): Calcd. for $CuC_{66}H_{98}N_{12}O_4$·3MeOH·H_2O: C, 63.68; H, 8.67; N, 12.91. Found, C, 63.99; H, 8.64; N, 12.78. Selected IR data (cm^{-1}): 2961, 2907, 2870, 1641, 1605, 1537, 1485, 1447, 1358, 1257, 1232, 1070, 1068, 997, 864, 8105, 795, 750, 702, 621.

[Cu(bdtbpza)$_2$(t-Bupy)$_4$] (2). Compound **2** was synthesized by a procedure similar to that used for **1** except that t-butylpyridine was used in place of pyridine. The color of reaction mixture was deep blue. Yield: 360 mg, 94 %. Elemental analysis (%): Calcd. for $CuC_{84}H_{130}N_{12}O_4$·3MeOH: C, 68.22; H, 9.34; N, 10.97. Found: C, 68.83; H, 9.26; N, 11.61. Selected IR data (cm^{-1}): 2957, 2905, 2870, 1618, 1549, 1462, 1425, 1358, 1277, 1229, 1070, 1031, 997, 843, 814, 795, 727, 673, 621.

[Cu(bdtbpza)$_2$(pym)$_2$(CH_3OH)$_2$] (3). Compound **3** was synthesized by a procedure similar to that used for **1** except that pyrimidine was used in place of pyridine. The solution became green-blue. Yield: 140 mg, 50%. Elemental analysis (%): Calcd. for $CuC_{58}H_{94}N_{12}O_6$: C, 62.27; H, 8.48; N, 15.03. Found: C, 61.79; H, 8.41; N, 14.86. Selected IR data (cm^{-1}): 2959, 2910, 2870, 1649, 1589, 1562, 1467, 1404, 1358, 1256, 1232, 1068, 1031, 997, 865, 816, 797, 750, 716, 689, 640, 621.

[Cu(bdtbpza)$_2$(eda)$_2$] (4). Compound **4** was synthesized by a procedure similar to that used for **1** except that ethylenediamine was used in place of pyridine. The solution became dark blue. Yield: 193 mg, 68%. Elemental analysis (%): Calcd. for $CuC_{52}H_{94}N_{12}O_4$•6H_2O: C, 55.62; H, 9.52; N, 14.98. Found: C, 55.53; H, 8.61; N, 14.79; Selected IR data (cm^{-1}): 3402, 3301, 3153, 2959, 2908, 2870, 1630, 1545, 1533, 1461, 1431, 1358, 1330, 1256, 1228, 1068, 1037, 997, 864, 816, 791, 756, 725, 657, 621.

[Cu(bdtbpza)$_2$(tmeda)(H_2O)$_2$] (5). Compound **5** was synthesized by a procedure similar to that used for **1** except that tetramethylethylenediamine was used in place of pyridine. The solution became deep blue. The violet solid thus formed during the reaction was filtered off, washed with small amounts of MeOH and dried under vacuum. Yield: 195 mg, 78%. Elemental analysis (%) Calcd. for $CuC_{54}H_{98}N_{10}O_6$: C, 64.17; H, 9.38; N, 13.86. Found: C, 64.48; H, 9.66; N, 13.94; Selected IR data (cm^{-1}): 3382, 2955, 2926, 2905, 2868, 1655, 1549, 1535, 1462, 1360, 1282, 1238, 1217, 1068, 1047, 1020, 995, 862, 817, 791, 768, 723, 694, 631, 621.

Crystallography

Single crystal X-ray diffraction data for **1**, **2** and **5** were collected at 100.0 (2) K on a Bruker SMART Apex CCD diffractometer using graphite monochromated Mo-Kα radiation (λ=0.71073 Å) while data for **3** and **4** were carried out on Brucker Kappa APEXII Crystal diffractometer at 200(2)K The structures were solved by direct methods and refined using full-matrix least-squares methods against F^2 values using the SHELXL-97 program included in the WINGX or SHELXTL

software package. The crystal structural determinations are detailed in the electronic supporting materials.

.

Acknowledgements

Authors are thankful to the Institute of Chemistry, Academia Sinica and National Science Council, Taiwan for their financial support. We thank Mr. Ting-Shen Kuo (Department of Chemistry, National Taiwan Normal University) for his assistance with the X-ray single-crystal structure analysis of complexes **3** and **4**. Special thanks to our colleague Jay-ar Dela Cruz and Dr Agnieszka J. Gordon (acgtranslation) for proofreading of our manuscript. Mass spectrometry analyses were performed by Mass Spectrometry facility of the Institute of Chemistry, Academia Sinica, Taiwan.

Notes and references

[a] Institute of Chemistry, Academia Sinica, Nankang, Taipei 105, Taiwan.

† Electronic Supplementary Information (ESI) available: IR spectra, EPR spectra and simulations; extinction coefficient for 3,5-DTBQ (calibration curve fitting); crystal packing figures of **1-5**. CCDC 999392 (**1**), CCDC 999395 (**2**), CCDC 999381 (**3**), CCDC 999383 (**4**) and CCDC 999385 (**5**) contain the supplementary crystallographic data. For ESI and crystallographic data in CIF or other electronic format see DOI: 10.1039/…….

1. (a)L. Que and W. B. Tolman, *Nature*, 2008, **455**, 333-340; (b)M. Fontecave and J. L. Pierre, *Coord. Chem. Rev.*, 1998, **170**, 125-140.
2. (a)E. T. Adman, *Adv. Protein Chem.*, 1991, **42**, 145-197; (b)H. Decker and N. Terwilliger, *J. Exp. Biol.*, 2000, **203**, 1777-1782; (c)C. Dennison, *Coord. Chem. Rev.*, 2005, **249**, 3025-3054; (d)S. Tardito and L. Marchio, *Curr. Med. Chem.*, 2009, **16**, 1325-1348.
3. J. E. Weder, C. T. Dillon, T. W. Hambley, B. J. Kennedy, P. A. Lay, J. R. Biffin, H. L. Regtop and N. M. Davies, *Coord. Chem. Rev.*, 2002, **232**, 95-126.
4. F. Tisato, C. Marzano, M. Porchia, M. Pellei and C. Santini, *Med. Res. Rev.*, 2010, **30**, 708-749.
5. E. V. Dikarev, K. W. Andreini and M. A. Petrukhina, *Inorg. Chem.*, 2004, **43**, 3219-3224.
6. (a)Y. F. Zeng, X. Hu, F. C. Liu and X. H. Bu, *Chem. Soc. Rev.*, 2009, **38**, 469-480; (b)C. B. Aakeroy, N. Schultheiss and J. Desper, *Dalton Trans.*, 2006, 1627-1635.
7. S. L. Li and T. C. W. Mak, *Struct. Chem.*, 1997, **8**, 49-63.
8. G. A. van Albada, I. Mutikainen, U. Turpeinen and J. Reedijk, *J. Chem. Crystallogr.*, 2004, **34**, 613-616.
9. C. Pettinari and S. Trofimenko, *Scorpionates II : chelating borate ligands*, Imperial College Press, London Hackensack, N.J., 2008.
10. N. Kitajima, K. Fujisawa, C. Fujimoto, Y. Morooka, S. Hashimoto, T. Kitagawa, K. Toriumi, K. Tatsumi and A. Nakamura, *J. Am. Chem. Soc.*, 1992, **114**, 1277-1291.
11. E. L. Hegg and L. Que, *Eur. J. Biochem.*, 1997, **250**, 625-629.
12. K. Valegard, A. C. T. van Scheltinga, M. D. Lloyd, T. Hara, S. Ramaswamy, A. Perrakis, A. Thompson, H. J. Lee, J. E. Baldwin, C. J. Schofield, J. Hajdu and I. Andersson, *Nature*, 1998, **394**, 805-809.
13. A. Otero, J. Fernandez-Baeza, J. Tejeda, A. Antinolo, F. Carrillo-Hermosilla, E. Diez-Barra, A. Lara-Sanchez, M. Fernandez-Lopez, M. Lanfranchi and M. A. Pellinghelli, *J. Chem. Soc. Dalton Trans.*, 1999, 3537-3539.
14. (a)A. Beck, A. Barth, E. Hubner and N. Burzlaff, *Inorg. Chem.*, 2003, **42**, 7182-7188; (b)A. R. Cowley, J. R. Dilworth and M. Salichou, *Dalton Trans.*, 2007, 1621-1629; (c)B. S. Hammes, M. T. Kieber-Emmons, J. A. Letizia, Z. Shirin, C. J. Carrano, L. N. Zakharov and A. L. Rheingold, *Inorg. Chim. Acta*, 2003, **346**, 227-238; (d)A. Beck, B. Weibert and N. Burzlaff, *Eur. J. Inorg. Chem.*, 2001, 521-527.
15. (a)B. Kozlevcar, P. Gamez, R. de Gelder, Z. Jaglicic, P. Strauch, N. Kitanovski and J. Reedijk, *Eur. J. Inorg. Chem.*, 2011, 3650-3655; (b)G. Turkoglu, C. P. Ulldemolins, R. Muller, E. Hubner, F. W. Heinemann, M. Wolf and N. Burzlaff, *Eur. J. Inorg. Chem.*, 2010, 2962-2974; (c)B. Kozlevcar, T. Pregelj, A. Pevec, N. Kitanovski, J. S. Costa, G. van Albada, P. Gamez and J. Reedijk, *Eur. J. Inorg. Chem.*, 2008, 4977-4982; (d)G. Turkoglu, F. W. Heinemann and N. Burzlaff, *Dalton Trans.*, 2011, **40**, 4678-4686.
16. G. B. Deacon and R. J. Phillips, *Coord. Chem. Rev.*, 1980, **33**, 227-250.
17. K. Nakamoto, *Infrared and Raman spectra of inorganic and coordination compounds*, 5th edn., Wiley, New York, 1997.
18. (a)B. Barszcz, T. Glowiak and J. Jezierska, *Polyhedron*, 1999, **18**, 3713-3721; (b)C. Place, J. L. Zimmermann, E. Mulliez, G. Guillot, C. Bois and J. C. Chottard, *Inorg Chem*, 1998, **37**, 4030-4039.
19. D. Kivelson and R. Neiman, *J. Chem. Phys.*, 1961, **35**, 149.
20. P. B. Sreeja, M. R. P. Kurup, A. Kishore and C. Jasmin, *Polyhedron*, 2004, **23**, 575-581.
21. I. M. Procter, B. J. Hathaway and P. Nicholls, *J. Chem. Soc. A*, 1968, 1678.
22. R. C. Chikate, A. R. Belapure, S. B. Padhye and D. X. West, *Polyhedron*, 2005, **24**, 889-899.
23. (a)A. Otero, J. Fernandez-Baeza, A. Antinolo, F. Carrillo-Hermosilla, J. Tejeda, A. Lara-Sanchez, L. Sanchez-Barba, M. Fernandez-Lopez, A. M. Rodriguez and I. Lopez-Solera, *Inorg. Chem.*, 2002, **41**, 5193-5202; (b)M. Porchia, G. Papini, C. Santini, G. G. Lobbia, M. Pellei, F. Tisato, G. Bandoli and A. Dolmella, *Inorg. Chim. Acta*, 2006, **359**, 2501-2508.
24. S. Youngme, N. Chaichit and K. Damnatara, *Polyhedron*, 2002, **21**, 943-950.
25. (a)R. Dulare, M. K. Bharty, S. K. Kushawaha and N. K. Singh, *J. Mol. Struct.*, 2011, **985**, 323-329; (b)V. Manriquez, M. CamposVallette, N. Lara, N. GonzalezTejeda, O. Wittke, G. Diaz, S. Diez, R. Munoz and L. Kriskovic, *J. Chem. Crystallogr.*, 1996, **26**, 15-22.
26. (a)N. V. Pervukhina and N. V. Podberezskaya, *J. Struct. Chem.*, 1985, **26**, 84-91; (b)H. Golchoubian, O. Nazari and B. Kariuki, *J. Chin. Chem. Soc.*, 2011, **58**, 60-68.

27. (a)E. Lay, Y. H. Song, Y. C. Chiu, Y. M. Lin, Y. Chi, A. J. Carty, S. M. Peng and G. H. Lee, *Inorg. Chem.*, 2005, **44**, 7226-7233; (b)K. Woo, H. Paek and W. I. Lee, *Inorg. Chem.*, 2003, **42**, 6484-6488; (c)G. Bandoli, D. Barreca, A. Gasparotto, R. Seraglia, E. Tondello, A. Devi, R. A. Fischer, M. Winter, E. Fois, A. Gambae and G. Tabacchi, *PCCP*, 2009, **11**, 5998-6007; (d)C. S. Hong, J. H. Yoon and Y. S. You, *Inorg. Chem. Commun.*, 2005, **8**, 310-313; (e)M. Lalia-Kantouri, A. G. Hatzidimitriou and D. Williams, *Z. Anorg. Allg. Chem.*, 2009, **635**, 2495-2502.

28. (a)A. Murphy, B. J. Hathaway and T. J. King, *J. Chem. Soc. Dalton Trans.*, 1979, 1646-1650; (b)B. Murphy, M. Aljabri, A. M. Ahmed, G. Murphy, B. J. Hathaway, M. E. Light, T. Geilbrich and M. B. Hursthouse, *Dalton Trans.*, 2006, 357-367; (c)A. Wojciechowska, A. Pietraszko, W. Bronowska, Z. Staszak, J. Jezierska and M. Cieslak-Golonka, *Polyhedron*, 2010, **29**, 2574-2581; (d)P. Stachova, M. Melnik, M. Korabik, J. Mrozinski, M. Koman, T. Glowiak and D. Valigura, *Inorg. Chim. Acta*, 2007, **360**, 1517-1522; (e)Z. D. Matovic, V. D. Miletic, M. Cendic, A. Meetsma, P. J. van Koningsbruggen and R. J. Deeth, *Inorg. Chem.*, 2013, **52**, 1238-1247.

29. J. Mukherjee and R. Mukherjee, *Inorg. Chim. Acta*, 2002, **337**, 429-438.

30. I. A. Koval, K. Sehmeczi, C. Belle, C. Philouze, E. Saint-Aman, I. Gautier-Luneau, A. M. Schuitema, M. van Vliet, P. Gamez, O. Roubeau, M. Luken, B. Krebs, M. Lutz, A. L. Spek, J. L. Pierre and J. Reedijk, *Chem. Eur. J.*, 2006, **12**, 6138-6150.

31. M. R. Malachowski, H. B. Huynh, L. J. Tomlinson, R. S. Kelly and J. W. F. Jun, *J. Chem. Soc. Dalton Trans.*, 1995, 31-36.

32. G. Speier, Z. Tyeklar, P. Toth, E. Speier, S. Tisza, A. Rockenbauer, A. M. Whalen, N. Alkire and C. G. Pierpont, *Inorg. Chem.*, 2001, **40**, 5653-5659.

33. J. Kaizer, T. Csay, G. Speier and M. Giorgi, *Journal of Molecular Catalysis a-Chemical*, 2010, **329**, 71-76.

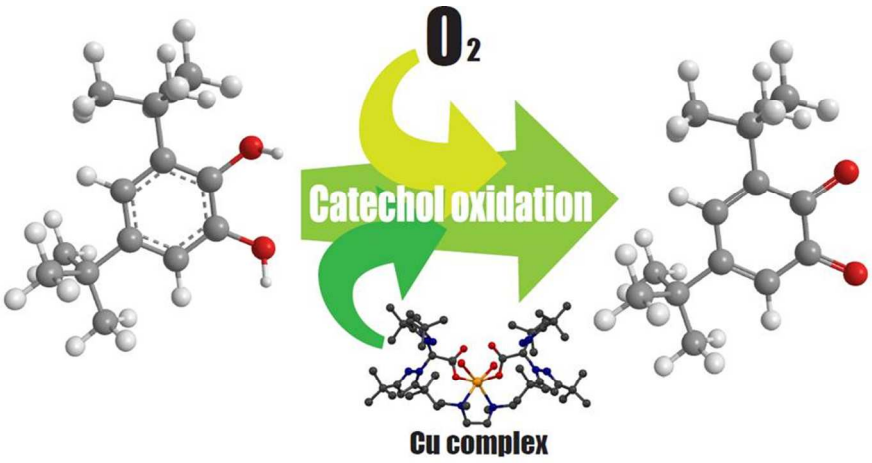

Heteroleptic copper(II) complexes containing bis(3,5-di-*t*-butylpyrazol-1-yl)acetate and nitrogen heterocyclic co-ligands identified influence of co-ligands on the conformation and catecholase-like catalytic activity.

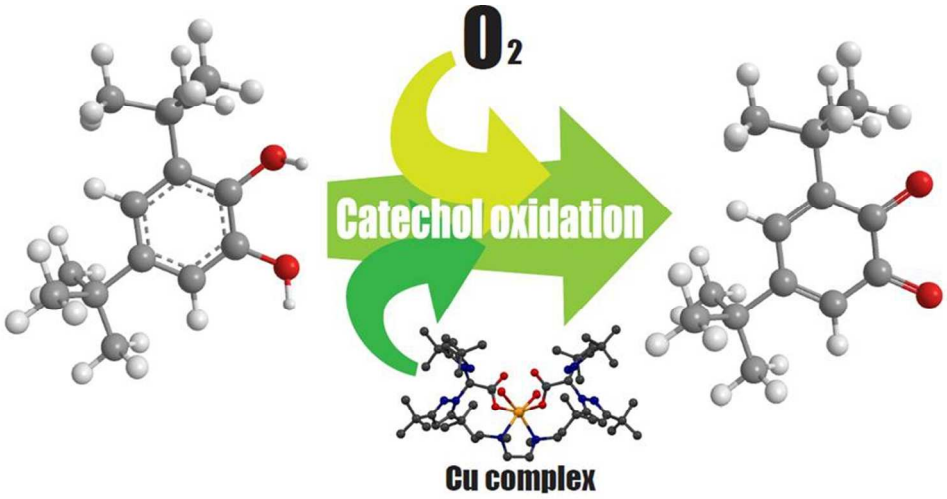

174x88mm (150 x 150 DPI)